`Supporting Information

A dysprosium(III)-based triple helical-like complex as a turn-on/off fluorescence sensor for Al(III) and 4,5-dimethyl-2-nitroaniline

Yi Yin[a], Rong Luo[a], Wen Wang[a], Rui Wang[a], Nan Jiang[a], Peng Chen[a], Hai-Jun Yu[a], Shuang-Yu Bi[b], Feng Shao*[a]

[a] *Key Laboratory of Marine Chemistry Theory and Technology, Ministry of Education, College of Chemistry and Chemical Engineering, Ocean University of China, Qingdao 266100, China*

[b] *State Key Laboratory of Microbial Technology, Shandong University, Qingdao 266237, China*

1 Experimental section

The ^{1}H NMR and FTIR of malondihydrazide and H_4L were shown in Figure S1, S2.

1.1 Synthesis of malondihydrazide

To the dimethyl malonate (4.30 mL, 37.60 mmol) in absolute EtOH (5 mL) was added hydrazine hydrate (7.29 mL, 150 mmol), and the solution refluxed for 10 h. The resulting white dihydrazide was filtered, given a cursory wash with ethanol, and then dried in vacuo. Yield: 47.20% (2.34 g) (based on dimethyl malonate). ^{1}H NMR (400 MHz, DMSO-d_6) δ 9.07 (s, 2H), 4.25 (s, 4H), 2.90 (s, 2H).

1.2 Synthesis of Schiff base ligand H_4L

3-ethoxysalicylaldehyde (0.83 g, 5 mmol) and a small amount of glacial acetic acid were added into the suspension of malonate (0.33 g, 2.5 mmol) in MeOH (20 mL), reflux for 6 h. The white precipitate of the desired dihydrazone was collected and washed with ethanol prior to drying in vacuo. Yield: 93.64% (1.00 g) (based on malondihydrazide). ^{1}H NMR (400 MHz, DMSO-d_6) δ 11.98 – 11.33 (m, 2H), 8.45 –

8.28 (m, 2H), 7.17 (dd, *J* = 35.4, 7.6 Hz, 2H), 6.95 (dd, *J* = 31.1, 6.0 Hz, 2H), 6.85 – 6.61 (m, 2H), 4.03 (td, *J* = 7.5, 7.0, 3.0 Hz, 4H), 3.34 (d, *J* = 13.8 Hz, 2H), 1.33 (tt, *J* = 6.8, 3.3 Hz, 6H).

1.3 Photoluminescence (PL) experiments

1.3.1 Photoluminescence spectrum

1@EtOH was prepared as a 10 μM solution, the test conditions were as follows: excitation wavelength 365 nm, slit width 5-10 nm, scanning range 400-700 nm.

1.3.2 PL lifetime kinetic

The light pulse was switched on at the 5th second and switched off at the 10th second, and the phosphorescence spectrum lifetime kinetic was collected over a period of 0-30 seconds.

1.4 The recycling experiments

For detecting Al^{3+}:

The complex **1** detecting Al^{3+} is not reversible due to their coordination reaction, which confirmed by MS-ESI.

For detecting DMNA:

(1) The complex **1** (10 mg) was dissolved in 10 mL ethanol, and the fluorescence spectrum was collected after ultrasound for 10 min.

(2) 1 mL DMNA (10^{-2} M) was added to the solution above, and fluorescence spectrum was recorded.

(3) Then the solvent (ethanol) was removed via rotavapor, and 1 mL ether was added and ultrasounded for 10 min (repeat 3 times) to remove the DMNA, the first cycling complex **1** was obtained by filtration and dried.

The second and third cycling complex **1** were obtained by repeating the procedures above for two and three times, respectively.

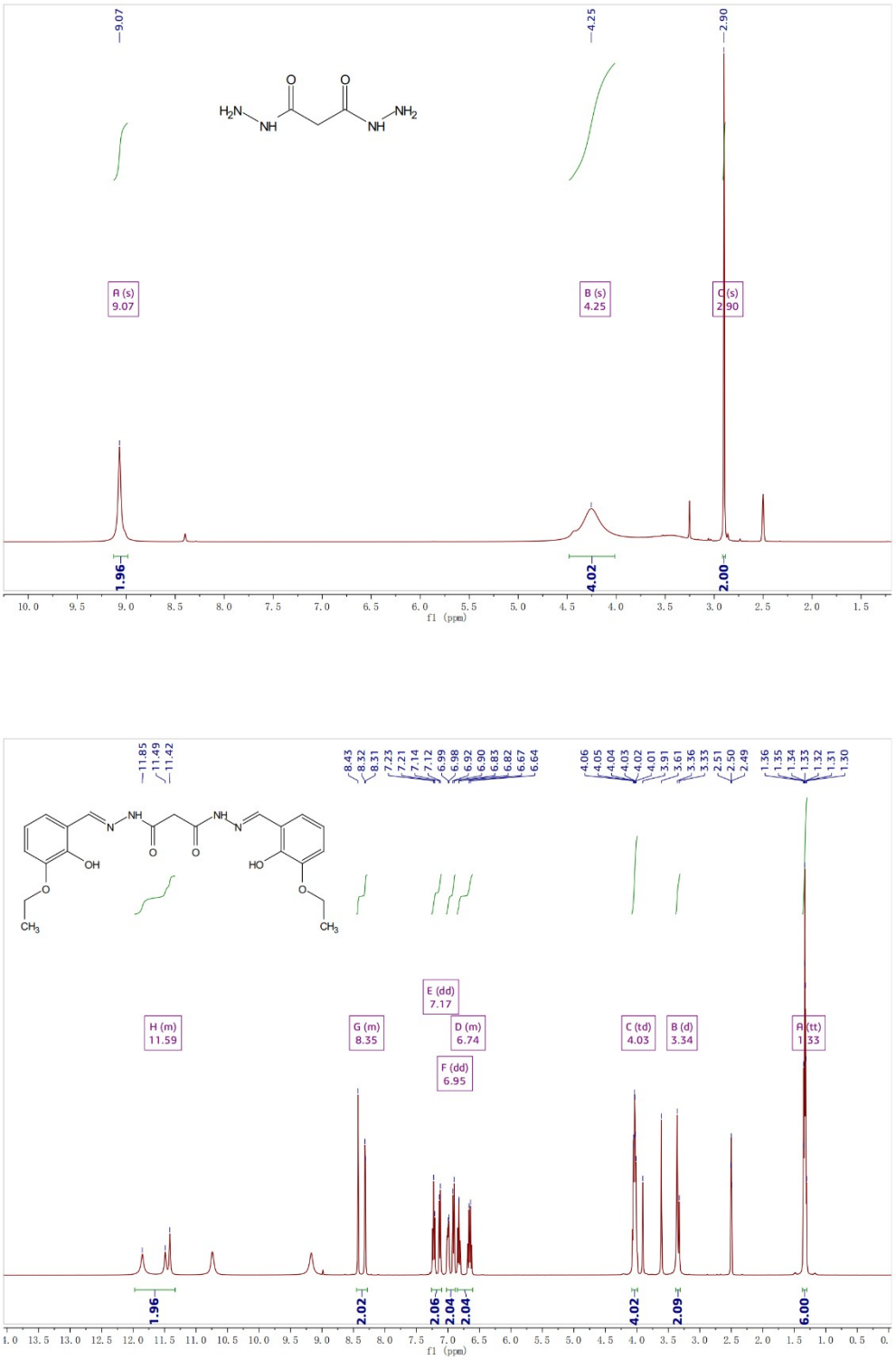

Figure S1 ^{1}H NMR of malondihydrazide (top) and H_4L (bottom).

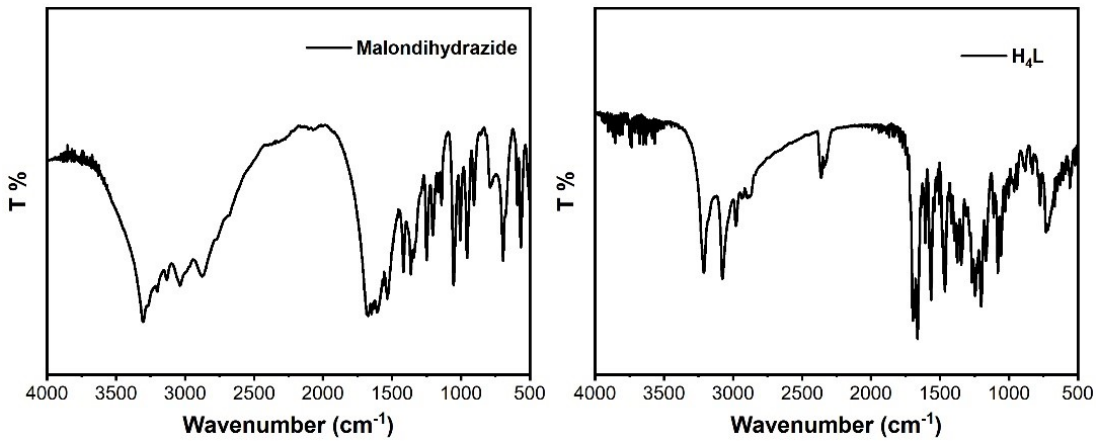

Figure S2 FTIR of malondihydrazide (left) and H_4L (right).

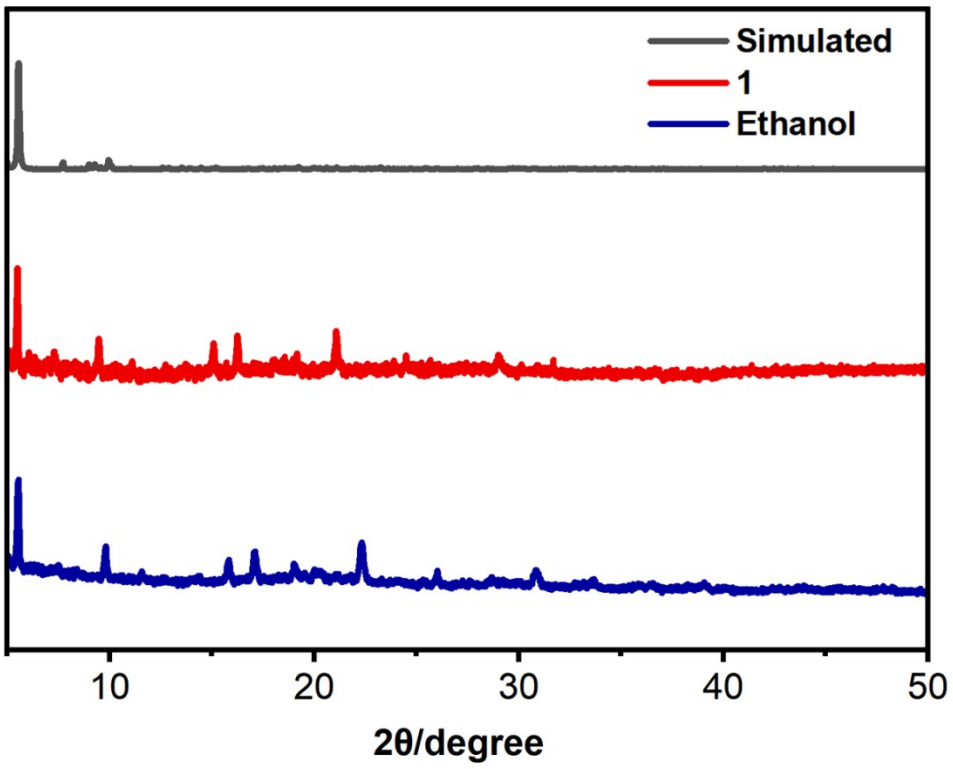

Figure S3 The powder X-ray diffraction patterns of **1**.

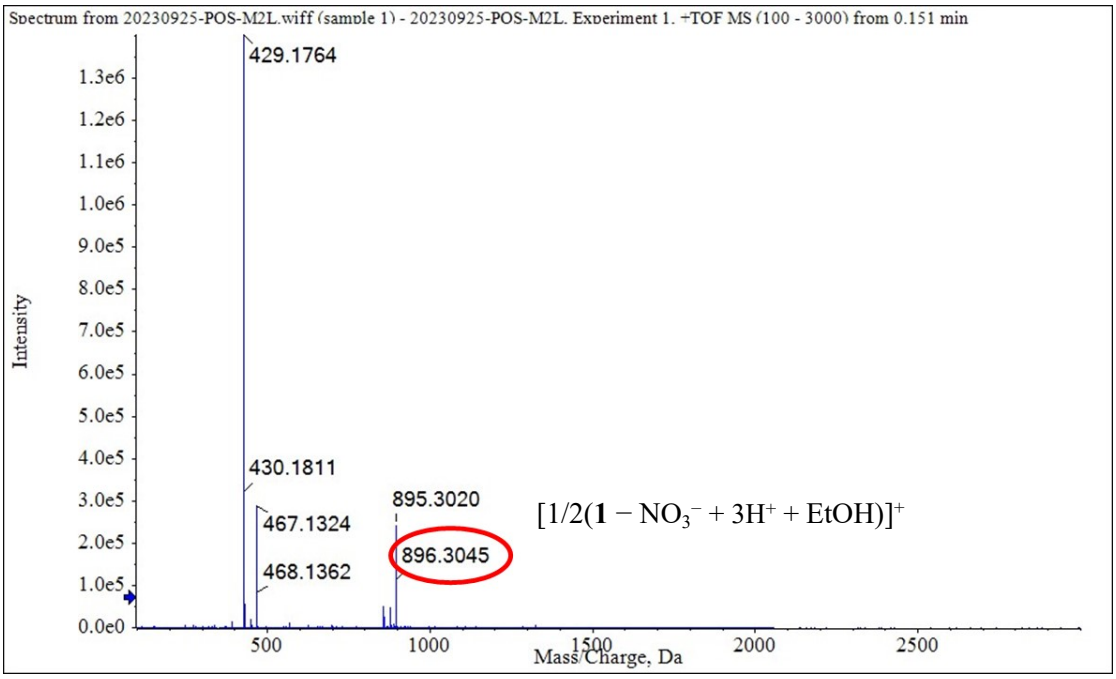

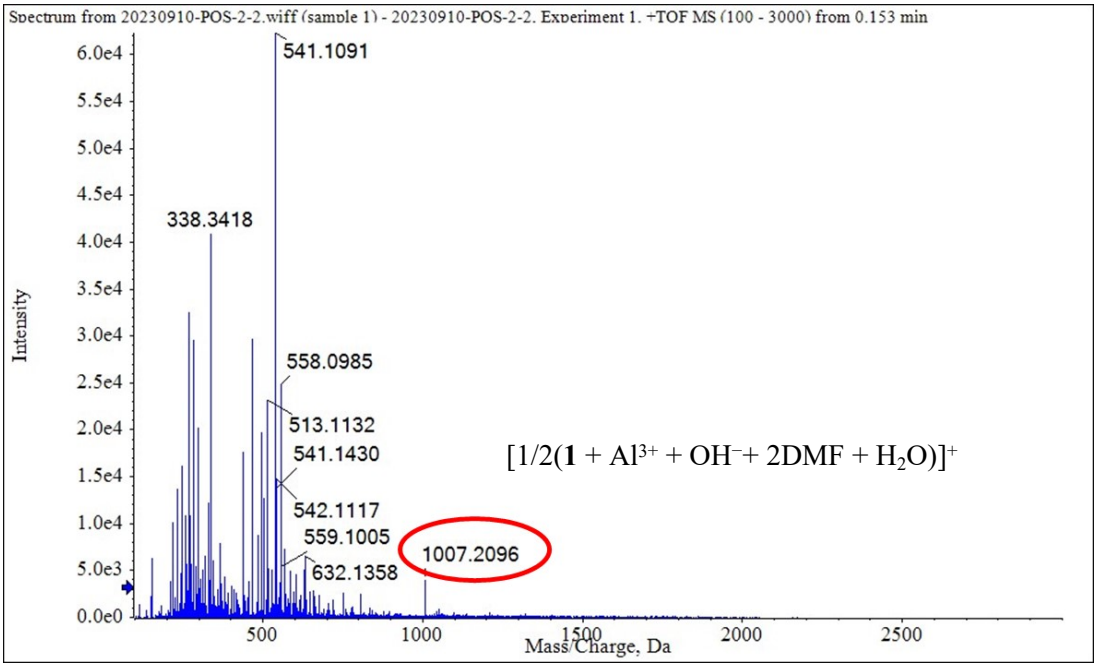

Figure S4 Mass spectrum of **1** (top,) and [**1**+Al^{3+}] complex (bottom).

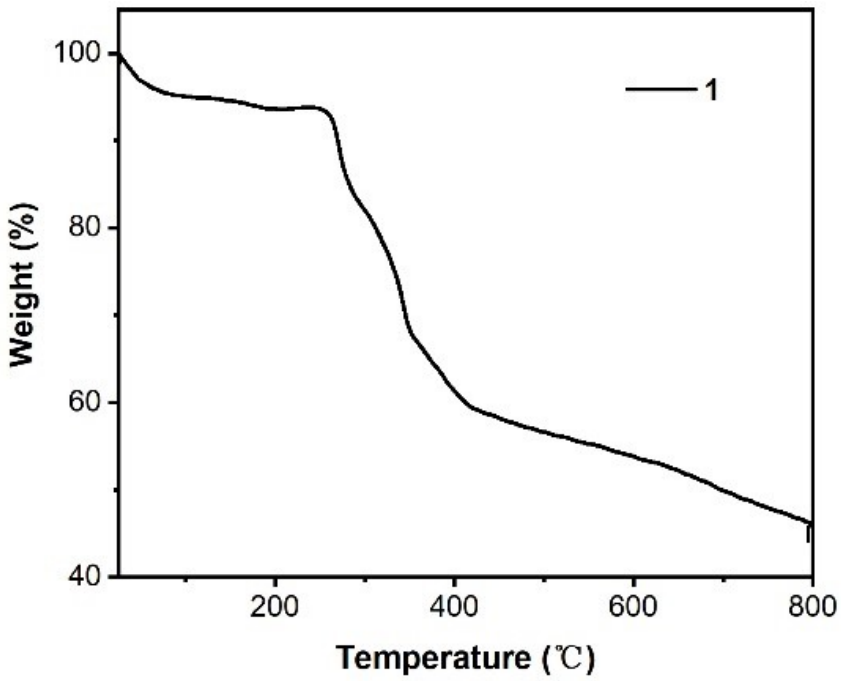

Figure S5 Thermogravimetric analysis (TGA) curve of **1**.

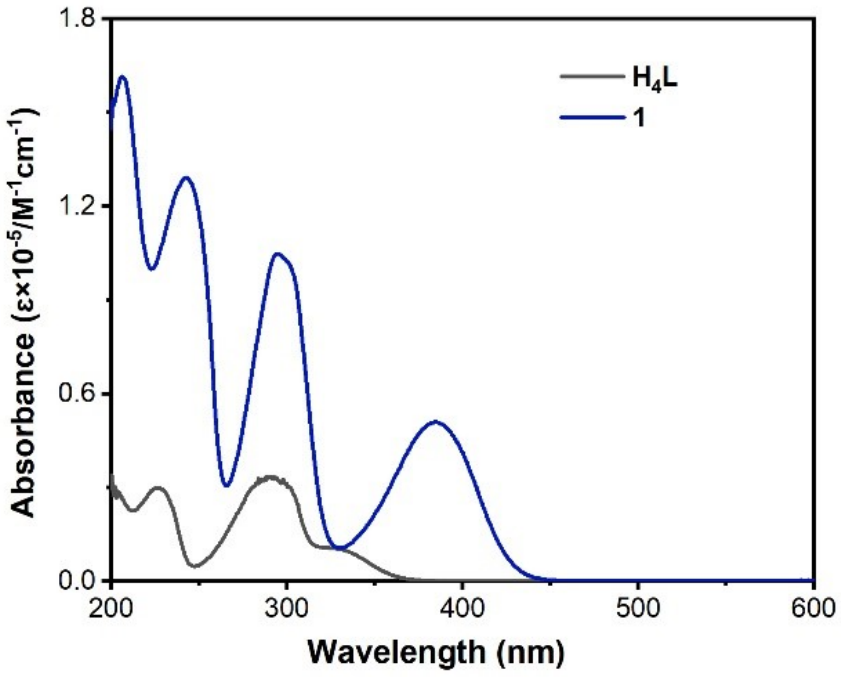

Figure S6 UV-Vis spectra of H_4L, **1@EtOH**.

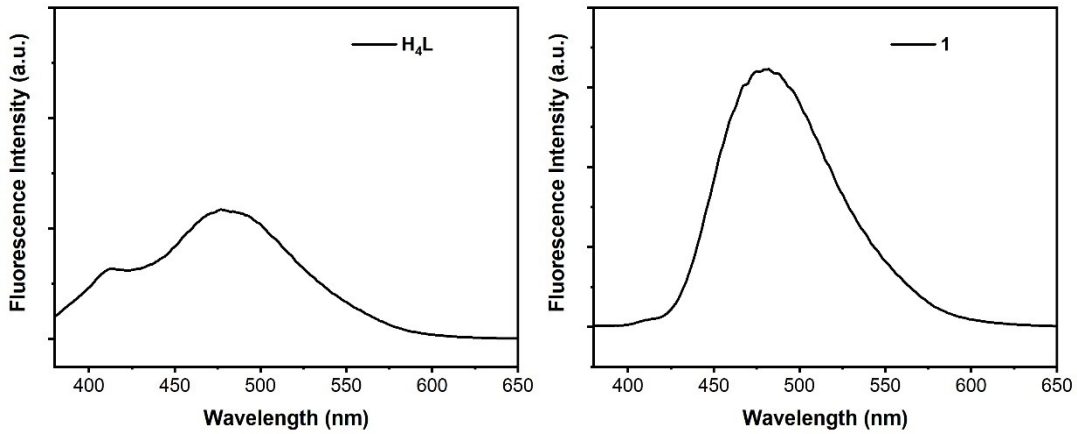

Figure S7 The emission spectra of H_4L and **1** in solid state at room temperature.

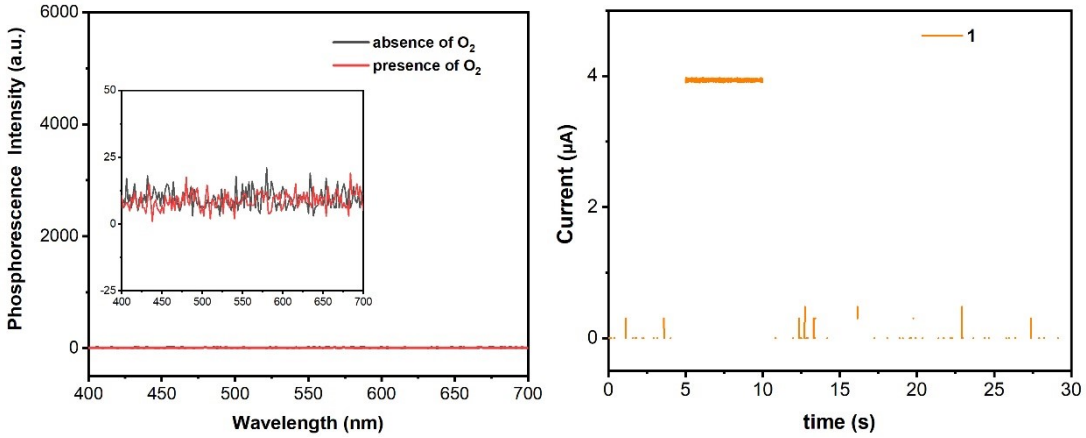

Figure S8 The PL spectra of **1@EtOH** in the presence and absence of O_2 (left) and the PL lifetime kinetic of **1@EtOH** in the absence of O_2 (right).

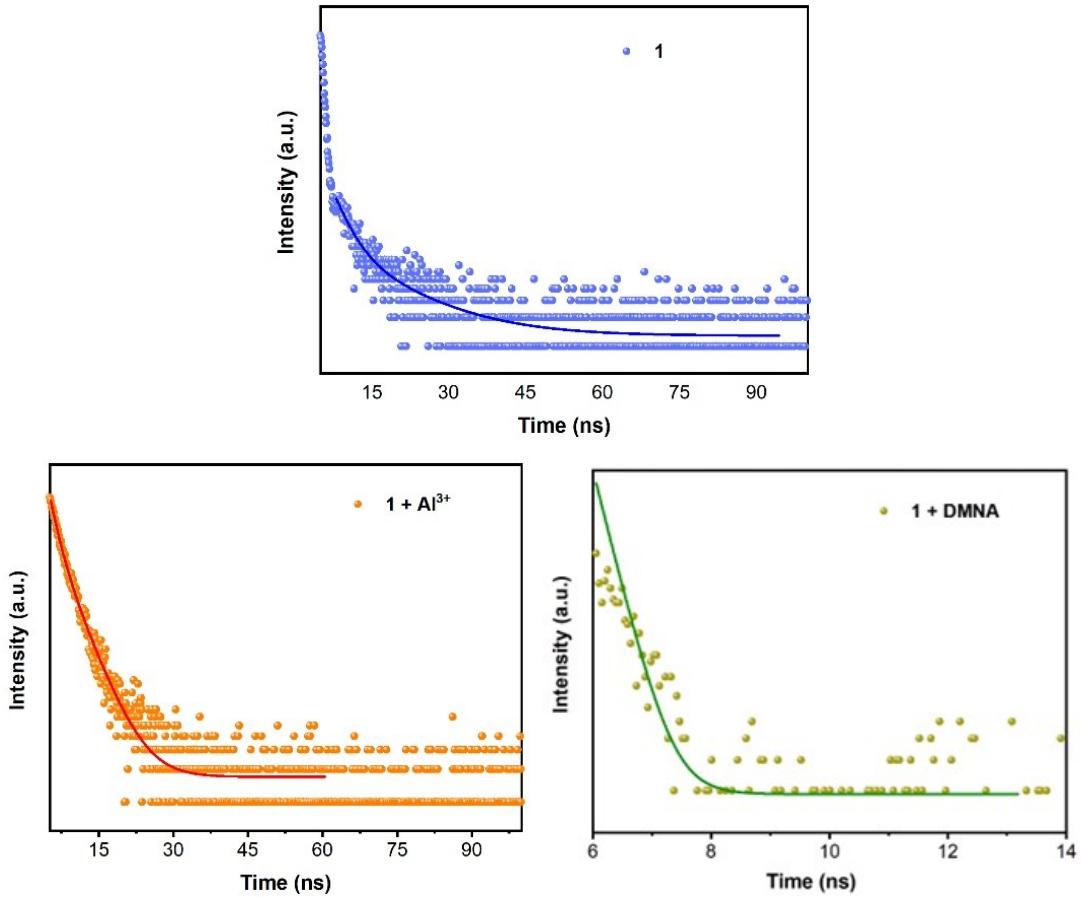

Figure S9 The time resolved luminescence decay corresponding fitted lines of **1@EtOH** (1.45 ns), [**1**+Al^{3+}] (2.99 ns) and [**1**+DMNA] (0.34 ns).

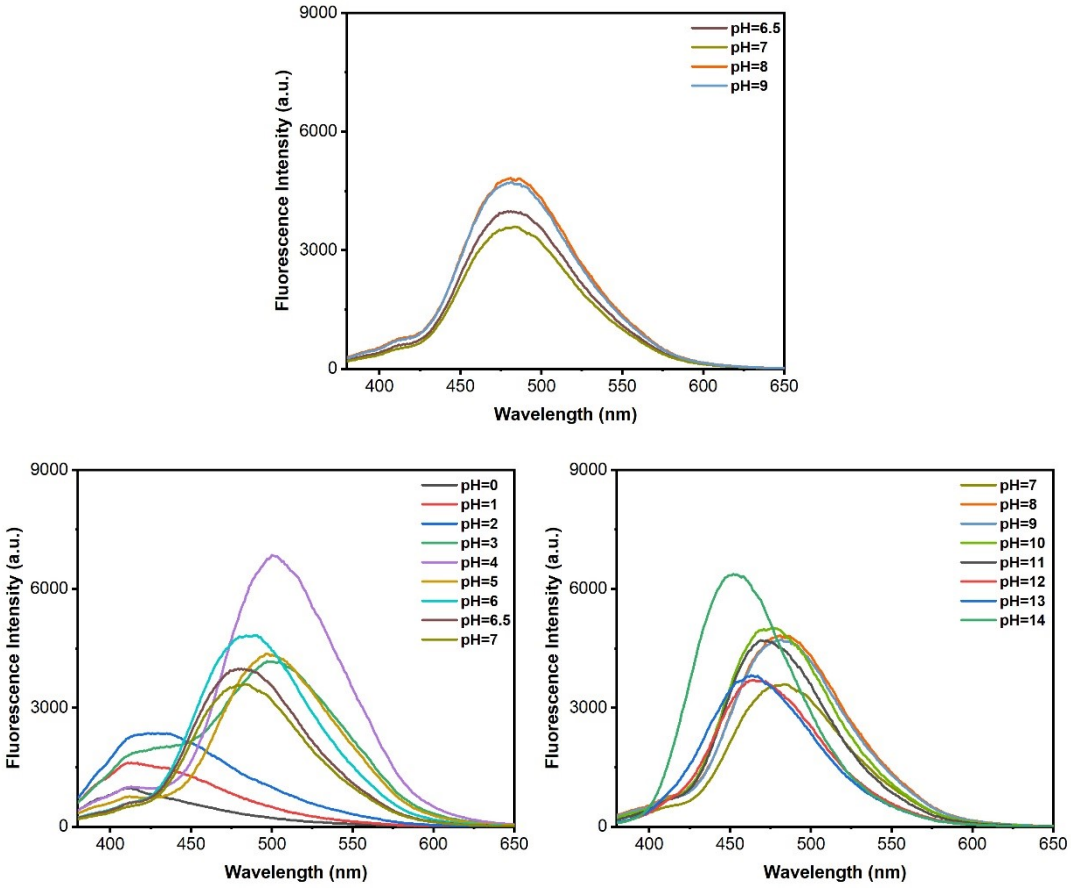

Figure S10 Fluorescence intensity of **1@EtOH** (10^{-5} mol L^{-1}) at different pH.

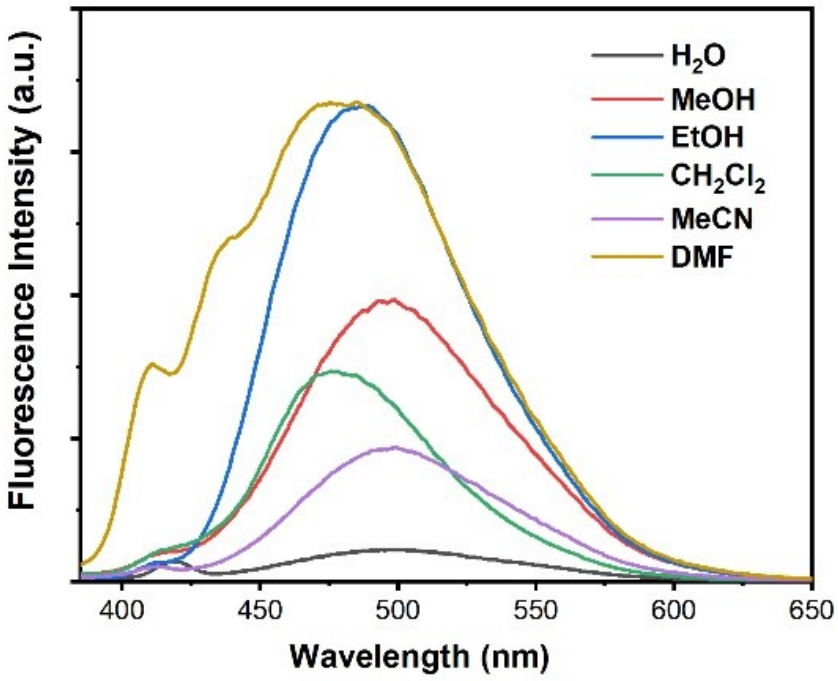

Figure S11 Fluorescence spectra of **1** in different solvents.

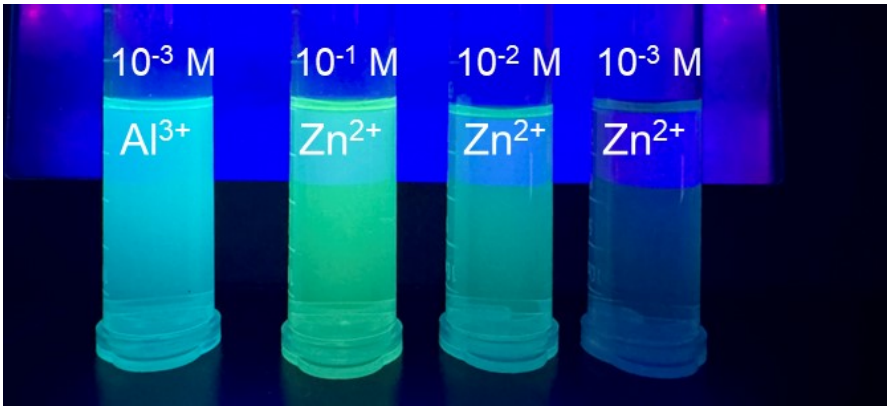

Figure S12 Photograph of fluorescent solutions under 365 nm UV light.

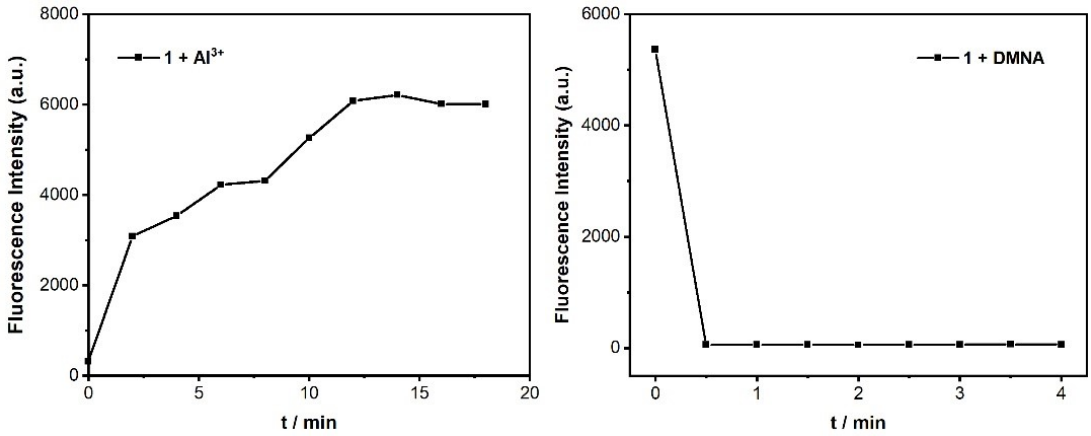

Figure S13 Time response of [**1**+Al^{3+}] and [**1**+DMNA].

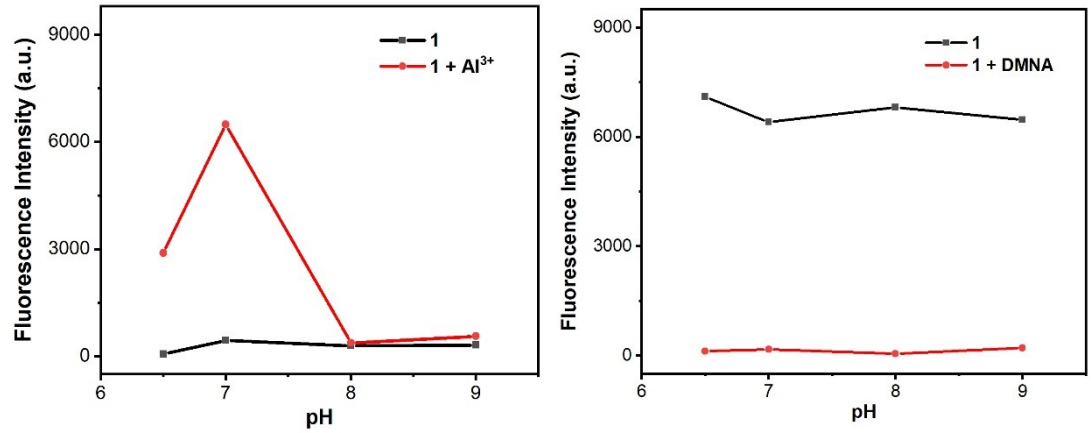

Figure S14 pH response of [**1**+Al^{3+}] and [**1**+DMNA].

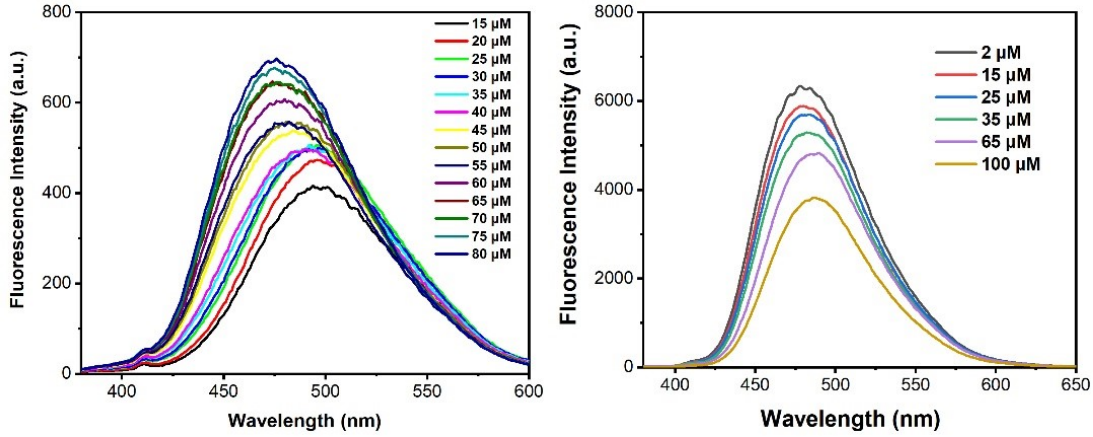

Figure S15 The emission spectra of **1@EtOH** after adding different concentrations of Al^{3+} and DMNA.

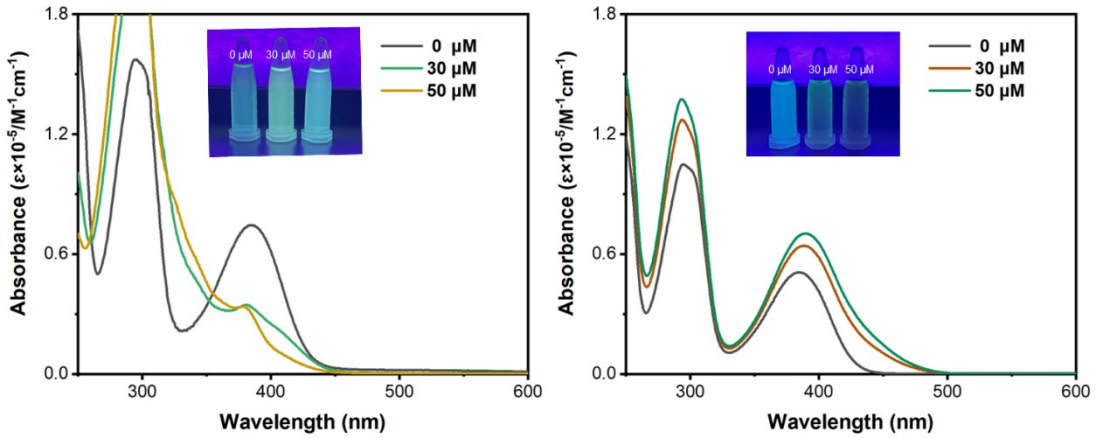

Figure S16 The UV spectra of **1@EtOH** after adding different concentrations of Al^{3+} (left) and DMNA (right).

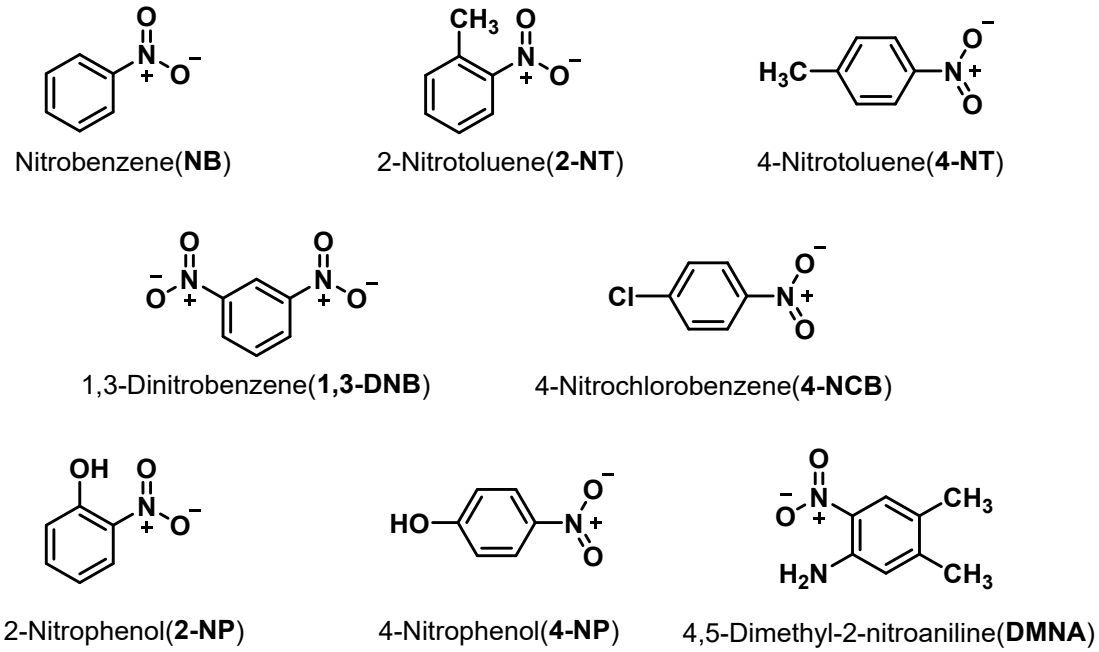

Figure S17 Chemical structures of NACs.

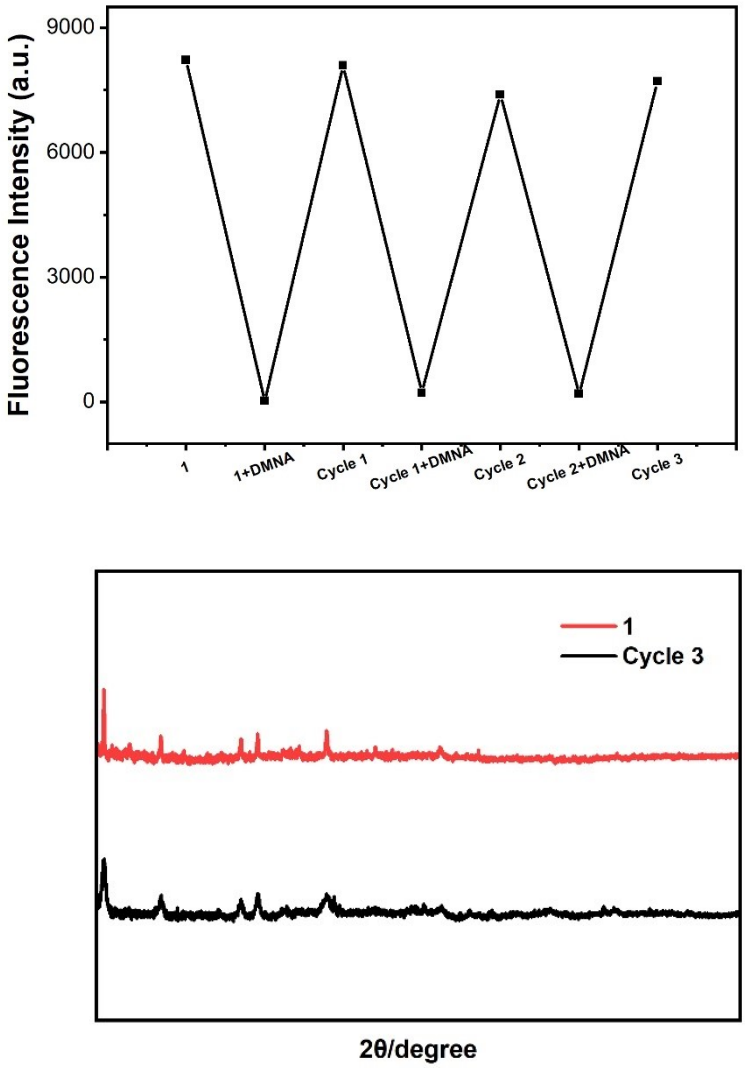

Figure S18 Changes in reversible fluorescence intensity during the cycle (top), PXRD data of the recovered recycled materials and compare with **1** (bottom).

Table S1 Selected bond lengths (Å) for **1.**

Selected bonds	Bond lengths (Å)
Dy1—O2	2.379(5)
Dy1—O4	2.431(5)
Dy1—O5	2.573(5)
Dy1—O6	2.563(5)
Dy1—O7	2.564(5)
Dy1—O8	2.392(5)
Dy1—N1	2.757(6)
Dy1—N4	2.782(6)
Dy1—N6	2.768(7)
Dy2—O10	2.596(5)
Dy2—O11	2.571(5)
Dy2—O12	2.566(5)
Dy2—O13	2.367(5)
Dy2—O14	2.389(5)
Dy2—O15	2.393(5)
Dy2—N8	2.768(6)
Dy2—N10	2.797(7)
Dy2—N12	2.762(6)
O3—K1	2.851(6)
O4—K1	2.864(6)
O15—K2	2.881(5)
O16—K2	2.836(6)

Table S2 Selected bond angles (°) for **1.**

Bond angles (°)		Bond angles (°)	
O2—Dy1—O4	78.73(18)	O13—Dy2—N10	63.82(18)
O2—Dy1—O5	92.57(18)	O13—Dy2—N12	141.21(17)
O2—Dy1—O6	124.13(17)	N8—Dy2—N10	113.08(18)
O2—Dy1—O7	148.56(17)	N12—Dy2—N8	118.40(19)
O2—Dy1—O8	81.57(19)	N12—Dy2—N10	123.59(18)
O2—Dy1—N1	78.80(19)	O2—K1—O1	52.30(15)
O2—Dy1—N4	64.67(17)	O2—K1—O3	117.78(17)
O2—Dy1—N6	145.74(19)	O2—K1—O4	65.57(16)
O5—Dy1—N1	59.94(17)	O2—K1—O9	99.5(2)
O5—Dy1—N4	72.87(17)	O3—K1—O1	109.88(17)
O5—Dy1—N6	119.71(17)	O3—K1—O4	54.43(15)
N1—Dy1—N4	117.83(19)	O3—K1—O9	122.8(2)
N1—Dy1—N6	125.73(19)	O9—K1—O1	127.3(2)
N6—Dy1—N4	111.58(18)	O13—K2—O14	65.69(15)
O10—Dy2—N8	59.64(18)	O13—K2—O15	64.08(16)
O10—Dy2—N10	63.14(17)	O13—K2—O16	118.78(18)
O10—Dy2—N12	129.20(16)	O13—K2—O17	97.05(18)
O13—Dy2—O10	89.15(16)	O13—K2—O18	120.01(17)
O13—Dy2—O11	153.19(17)	O13—K2—O20	156.10(19)
O13—Dy2—O12	122.74(19)	O16—K2—O15	57.44(15)
O13—Dy2—O14	78.21(17)	O16—K2—O17	124.82(18)
O13—Dy2—O15	77.35(18)	O16—K2—O20	84.21(18)
O13—Dy2—N8	83.41(18)	O17—K2—O20	72.01(18)

Table S3 SHAPE analysis of eight-coordinated and nine-coordinated geometry for **1**.

Label Symmetry	Dy	Label Symmetry	K
EP D_{9h}	34.675	OP D_{8h}	41.387
OPY C_{8v}	23.23	HPY C_{7v}	31.723
HBPY D_{7h}	17.626	HBPY D_{6h}	31.317
JTC C_{3v}	11.935	CU O_h	31.655
JCCU C_{4v}	9.337	SAPR D_{4d}	32.244
CCU C_{4v}	8.619	TDD D_{2d}	30.617
JCSAPR C_{4v}	2.945	JGBF D_{2d}	26.74
CSAPR C_{4v}	2.584	JETBPY D_{3h}	31.475
JTCTPR D_{3h}	2.382	TBTPR C_{2v}	29.298
TCTPR D_{3h}	2.083	BTPR C_{2v}	30.295
JTDIC C_{3v}	7.838	JSD D_{2d}	30.42
HH C_{2v}	10.723	TT T_d	30.029
MFF C_s	2.49	ETBPY T_d	29.803

Abbreviations: EP – Enneagon, OPY − Octagonal pyramid, HBPY − Heptagonal bipyramid, JTC − Johnson triangular cupola J3, JCCU − Capped cube J8, CCU − Spherical-relaxed capped cube, JCSAPR − Capped square antiprism J10, CSAPR − Spherical capped square antiprism, JTCTPR − Tricapped trigonal prism J51, TCTPR − Spherical tricapped trigonal prism, JTDIC − Tridiminished icosahedron J63, HH − Hula-hoop, MFF – Muffin, OP − Octagon, HPY − Heptagonal pyramid, HBPY − Hexagonal bipyramid, CU − Cube, SAPR − Square antiprism, TDD − Triangular dodecahedron, JGBF − Johnson gyrobifastigium J26, JETBPY − Johnson elongated triangular bipyramid J14, JBTPR − Biaugmented trigonal prism J50, BTPR − Biaugmented trigonal prismJSD − Snub diphenoid J84, TT − Triakis tetrahedron, ETBPY − Elongated trigonal bipyramid.

Table S4 The summary of the detection limits of Al^{3+} by various fluorescent probes.

Number	Probe	Detection limit / μM
1	BHMMP [1]	0.7
2	Tb-MOF [2]	6.10
3	QCT@ZIF-8 [3]	0.58
4	HL [4]	0.84
5	HPU-24@Ru [5]	11.63
6	Tb@MOF-808-TDA [6]	0.08
7	MOF **1** [7]	2.90
8	This work	0.53

Table S5 Double exponential function for [1+Al^3].

$$\left(A_1 \times t_1^2 + A_2 \times t_2^2\right) \div \left(A_1 \times t_1 + A_2 \times t_2\right)$$

A_1	469.36
t_1	1.94 ns
A_2	127.95
t_2	4.62 ns
[1+Al^3]	2.99 ns

References

1. Z. Xing, J. Wang, J. Huang, X. Chen, Z. Zong, C. Fan and G. Huang, *Molecules*, 2022, **27**, 2569-2583.

2. X. Jing, J. Liu, M. Guo, G. Chen, G. Ren, J. Li, H. Qin, Z. Yao, Y. Wan, W. Song, H. Zeng, F. Yang, D. Zhao and K. Hu, *New J. Chem.*, 2023, **47**, 13619−13626.

3. T. Zhong, F. Sun, Z. Zhang and G. Wang, *J. Photoch. Photobio. A: Chem.*, 2023, **440**, 114677-114682.

4. G. C. Das, A. Kumar Das, D. Das, T. Raj Maity, A. Samanta, F. Ali Alasmary, A. Salem Almalki, A. Iqbal and M. Dolai, *J. Photoch. Photobio. A: Chem.*, 2023, **440**, 114663-114672.

5. H. Li, Y. Wang, F. Jiang, M. Li and Z. Xu, *Dalton Trans.*, 2023, **52**, 3846-3854.

6. D. Mei and B. Yan, *ACS. Appl. Mater. Interfaces*, 2023, **15**, 16882-16894.

7. X.-C. Huang, Y.-X. Jiang, Z.-J. Han, W. Yong, Q.-X. Huang, W.-X. Shi, X.-R. Chen, J.-J. Kong and H. Wu, *J. Mol. Struct.*, 2023, **1289** 135897-135905.